J Mater Sci
DOI 10.1007/s10853-012-6642-5

Hydration-induced reinforcement of rigid polyurethane–cement foams: mechanical and functional properties

Letizia Verdolotti · Ernesto Di Maio · Marino Lavorgna · Salvatore Iannace

Received: 11 April 2012 / Accepted: 5 June 2012

Abstract Mechanical and functional properties of a newly proposed hybrid foam based on rigid polyurethane foam and Portland cement for application in the building field are herein reported. The hybrid is characterized by the co-continuity of the two phases, hydrated cement and polyurethane, which cooperate in a synergistic way to the properties of the resulting material. Furthermore, the closed-cell foam structure gives the material properties typical of porous materials: in particular, the hybrid foam evidences thermal insulation, sound absorption and acoustic insulation, high impact energy and low density typical of polymeric foams. At the same time, the hybrid foam exhibits water vapor permeability, improvement of thermal stability, high compressive mechanical behavior, and adhesion to concrete and mortars typical of inorganic binders such as cement. The materials were obtained by mixing cement powder with polyurethane foam precursors, i.e., methylene di(phenyl-isocyanate), polyol polyether and catalysts, and silicone surfactants. Water was used as blowing reagent. The resulting compounds were foamed in flat closed molds. The cement phase was then allowed to hydrate in accelerated conditions, i.e., in water at 60 °C for 72 h. Mechanical, morphological, and functional characterization showed that the hydrated cement particles interacted with each other, forming an inorganic network within the polymeric matrix (co-continuity), thus "hydration-induced reinforcement of polymer–cement" hybrid foam, in contraposition with the term "composite foam."

L. Verdolotti · M. Lavorgna · S. Iannace
Institute for Composite and Biomedical Materials, National Research Council (IMCB-CNR), P.le Tecchio 80, 80125 Naples, Italy

E. Di Maio (✉)
Department of Materials and Production Engineering, University of Naples Federico II, P.le Tecchio 80, 80125 Naples, Italy
e-mail: edimaio@unina.it

Introduction

Polyurethane (PU) foams are among the most important and diffuse plastic materials for the excellent insulating and cushioning characteristics. However, their low strength and stiffness impede their use as structural materials in the building field [1, 2]. To overcome this problem, in the scientific and technological literature, there can be found numerous strategies aimed to the increase of the mechanical properties of PU foams, mostly by filling the polymeric matrix with a rigid phase. Reinforced PU foams have been prepared with several kinds of fillers, such as glass fibers [3, 4], nano-silica [5, 6], wood flours [7], clays [6, 8], and carbon powder [9]. These studies point out the problem of adhesion between the polymeric matrix and the filler for mechanical applications. In particular, at high filler content (i.e., more than 30 wt%), the overall behavior of the PU foam may shift from ductile to brittle, as a consequence of the incomplete bonding of the filler to the polymeric matrix. Thus, while the filler may act to stiffen the foam, the individual particles can act as pre-existing flaws, allowing for easier crack initiation and propagation, thereby decreasing deformation and strength. Pre-treatments of the filler have been successfully performed to improve the adhesion [2, 5, 6, 8] although increasing material cost.

In this context, we have recently introduced a new type of lightweight hybrid material based on PU foam and hydrated cement in which both the inorganic and the organic phases are co-continuous throughout the material and the phases are finely and intimately dispersed within

Published online: 19 June 2012

each other [10–12]. The system is designed to meet both the advantages of the PU foams and the inorganic binder, to achieve a material which evidences thermal and acoustic insulation, high impact energy and low density typical of the PU foams and water vapor permeability, fire resistance, high compressive mechanical behavior, and adhesion to concrete and mortars typical of inorganic binder cement.

In [11], the hybrid was based on a PU formulation typical of flexible foams and the achieved cellular structure was an open-celled one. In particular, in the cited paper, emphasis was given to the chemical characterization of this new class of materials, and the occurrence of the hydration reaction has been evidenced via wide-angle X-ray diffraction (XRD), chemically bonded water, and scanning electron microscope analyses. In [12]; a new hybrid based on a formulation typical of rigid PU foams (characterized by a closed-celled structure, to enhance the structural characteristic and the thermal insulating properties) has been studied. The occurrence of co-continuity between the two (organic and inorganic) phases has been proved by means of solvent swelling and preliminary mechanical testing and a new class of materials was thereby defined as "hydration-induced reinforcement of polymer–cement" (HIRP-C) hybrid foam.

In the present paper, we extend the mechanical characterization of these materials and report several functional properties of interest in the building field, such as thermal insulating properties, acoustic insulation and absorption properties, water vapor transmission, and dimensional stability.

Experimental

Materials

Polyol polyether and diphenylmethane di-isocyanate (MDI) were kindly supplied by Huntsman Tioxide Europe (Ternate, Italy); catalysts, chain extenders, and silicone surfactants were supplied by Momentive Performance Materials (Leverkusen, Germany). Portland cement in powder form (CEM type IIA-S class 42,5R) was supplied by CEMENTIR Holding (Spoleto, Italy). The chemicals were used as received. Distilled water was utilized as chemical blowing agent.

Methods

Samples preparation

Samples were prepared by mixing at room temperature the cement powder to the polyol with catalysts, silicone surfactant, chain extenders, and water as blowing agent. This mixture was stirred mechanically for 2 min and then MDI was added and mixed for 40 s. Mixing was performed according to ASTM C305 using a Hobart mixer (mod. N50, Hobart, Canada). According to [10], the polyurethane/cement weight ratio was fixed to 2/3. After mixing all the components, the mixture was poured in a wood closed mold ($50 \times 50 \times 5$ cm^3) and the foam was allowed to expand/cure for 20 min at room temperature. The sample was then removed from the mold. Neat polyurethane formulation (e.g., without cement, Neat PUR) was also produced for proper comparison. Selected samples were cured in water, for 72 h at 60 °C, to allow for the hydration of cement powder. Both hydrated (hydration induced reinforced polymer–cement, thereafter referred to as "HIRP-C") and un-hydrated (polymer–cement, thereafter referred to as "P–C") samples were subjected to chemical, physical, mechanical, and morphological characterization. Important functional properties specific for the building field were analyzed too. Table 1 reports the compositions of the materials produced and the adopted classification.

Degree of hydration

To evaluate the degree of hydration of the cement, samples were milled with acetone and ethyl ether twice to stop the hydration reactions. The degree of hydration was determined from the water content (chemically bonded water—H_2O_{cb}) of the hydrated samples according to ASTM C114, as described in [11], with the assumption that the chemically bonded water can be estimated by assuming a value equal to 32 wt% for fully hydrated cement, cured at 25 °C for 28 days in water, and equal to 23 wt% for the cement sample cured in water at 60 °C for 72 h. This difference is due to the limited hydration of the larger cement grains (>15 μm) at higher temperatures [13, 14].

X-ray diffraction

The mineralogical composition (mineral phases) of hybrids has been investigated by XRD. Mineralogy was performed

Table 1 Composition and adopted classification of samples

Sample	Polyurethane (wt%)	Cement (wt%)	Density (kg/m^3)
Neat PUR	100	0	170
P-C2	40	60	200
P-C3	40	60	300
P-C4	40	60	370
P-C7	40	60	750
HIRP-C2	40	60	230
HIRP-C3	40	60	320
HIRP-C4	40	60	400
HIRP-C7	40	60	800

on milled samples at room temperature using a Philips X-ray generator and a Philips diffractometer, type PW1710 (Philips, Holland). The X-ray beam was nickel-filtered Cu-K_α radiation of wavelength 1.54 Å operated at the generator voltage of 40 kV and current of 20 mA. The diffraction intensity data were collected automatically at a scanning rate of 0.6°/min with 0.01°/s steps.

Density

Densities, reported in Table 1, were calculated as the ratio between the final foam weight (as measured with an analytical balance) and volume (as measured by a high resolution caliper) of cylindrical samples obtained from the panels extracted from the mold.

Microstructural analysis

For microstructural analysis, the foamed samples were analyzed by scanning electron microscopy (SEM). The samples were first sectioned using a razor blade and then coated with gold using a sputter coater (mod. SC500, Emscope, UK). The morphology of the fracture surface was studied using a SEM (mod. S440, Leica Microsystems GMbH, Germany) operating at 20 kV.

Water vapor permeability

Water vapor transmission properties were analyzed according to UNI EN 12086. Samples 110 mm in diameter and 25-mm thick are exposed form one side to 85 % RH and to the other to 0 % RH. The weight change of the cylinder containing the sample is recorded. After a transient period, a linear weight change is achieved and absolute water vapor permeability, δ, is calculated as

$$\delta = \frac{Gd}{A\Delta p},$$

where G is the slope of the weight versus time curve, d is the thickness of the sample, A is the area of the surface exposed to the vapor flux, and Δp is the difference in the water vapor partial pressure. Finally, the resistance to the water vapor permeation, μ, is calculated as

$$\mu = \frac{\delta_{\text{air}}}{\delta},$$

where δ_{air} is the water vapor permeability of air equal to 1.94×10^{-10} kg m^{-1} s^{-1} Pa^{-1} at 23 °C.

Dimensional stability

Dimensional stability of the different materials has been measured using ASTM D2126, which is specific for rigid cellular materials. Samples are conditioned for 24 h at different conditions: 70 °C, 20 % RH; 100 °C, 20 % RH; 38 °C, 100 % RH; and 70 °C, 100 % RH. Results are described as dimensional changes, Δl, calculated as

$$\Delta l(\%) = \frac{l_{\text{f}} - l_0}{l_0} \times 100,$$

where l_{f} and l_0 are final and initial measures, respectively.

Adhesion test

Adhesion of the hybrids to mortars was studied trough tensile peel test according to UNI-EN 1015-12 and it consists in the measure of the adhesive force between the mortar and the testing material. Tensile force is applied using an iron cylinder 110 mm in diameter, glued with epoxy resin (Superflex, Kerakoll S.p.A. Sassuolo, MO, Italy) to 10-mm thick layer of mortar previously deposited on the HIRP-C, the P–C or the Neat PUR, and cured for 14 days at room temperature and 100 % RH.

Thermal insulating properties

Thermal conductivity was measured using a Lambda Heat Flow Meter (mod. HFM 436, Netzsch, Germany), according to ASTM C518-04. The test has been conducted on a slab 100 × 100 mm^2 by imposing a temperature gradient, ΔT, across the thickness, d, of the sample (in the range 20–63 mm) and by measuring the resulting heat flux, Q. According to the Fourier law for heat conduction, the thermal conductivity, λ, can be hence evaluated by

$$\lambda = \frac{Q}{A}\frac{\Delta T}{d}.$$

Acoustic properties

Sound absorption coefficient (α) was measured for selected samples according to the standard UNI EN 10534, using an impedance Kundt tube, 100 mm in diameter and 570 mm in length. The distance between first microphone and samples was 200 mm, while the distance between first and second microphone was fixed at 50 mm. The frequency ranged from 200 to 1,800 Hz. The signal (white noise) is generated by a loudspeaker placed at one end of the tube, while the samples are placed on a rigid surface at the opposite end. Thicknesses of samples were 10, 25, and 50 mm.

Acoustic insulation properties [transmission loss (TL)] for selected samples were measured according to UNI EN ISO 11654-717. The analysis was performed on a rectangular panel (dimensions 170 × 90 × 5 cm^3 $L \times W \times T$) which was placed as a separation between a reverberant room, where a uniform acoustic field is artificially

generated, and an anechoic room, where the transmitted acoustic field (by the panel vibrations) was measured. In the reverberant room, a rotating microphone provided the pressure level frequency spectrum and allowed to control, in the frequency range considered, the pressure level and its uniform spatial distribution. The acoustic characterization was carried out in the frequency range 100–10,000 Hz and numerical results are grouped in 1/3-octave bands.

Thermal properties (TGA)

The thermal degradation of the Neat PUR, composite, and hybrid foams has been investigated by thermogravimetric (TGA) and derivative TGA (DTG) analyses. The tests have been carried out on a TGA2950 (TA Instruments, USA) under air atmosphere. The samples were heated on platinum pans from 30 up to 1,000 °C by applying a heating rate of 10 °C/min.

The TGA experiments were performed on selected foam samples to analyze the effect of the cement and the hydrated cement on thermal degradation process of polyurethane. In particular, the DTG in the 400–550 region temperature was deconvoluted, for hybrids, by means of the best fits by Gaussian sum to evidence the contribution of cement hydrated phases.

Mechanical properties

Compressive tests were carried out on a SANS testing machine (mod. CMT4304, Shenzhen SANS Testing Machine Co., China) with a 30 kN load cell, according to ASTM D1621.

Results and discussion

Degree of hydration

The values of chemically bonded water (H_2O_{cb}) for several hybrids are reported in Table 2. The values were normalized with the amount of cement in the different samples (60 %). The hybrids (HIRP-Cs) showed, after 72 h of hydration, an amount of H_2O_{cb} ranging from 17 to 21 wt% which is lower than 23 wt%, the theoretic limit for neat cement. This result could be explained by recalling the hydrophobic character of the polyurethane matrix surrounding the cement particles. In fact, the hydration of cement particles is occurring within the struts and walls of the porous hybrids, partially constituted of polyurethane [13, 14].

Table 2 Chemically bonded water for selected samples

Sample	H_2O_{cb} wt% with respect to cement content (60 %)
Neat PUR	0
HIRP-C2	17
HIRP-C3	17
HIRP-C4	20
HIRP-C7	21
Neat cement	23

Percentages are given with respect to quantity of cement actually present in the samples

X-ray diffraction

XRD investigation was performed to evaluate the occurrence of hydration of the cementitious phases within the hybrids and to clearly distinguish the composites, where cement remains in the anhydrous state, from the hybrids, where cement hydration resulted in the formation of amorphous hydrated calcium silicate phase (CSH), in turn allowing for the dramatic changes in functional as well as mechanical properties of the materials. According to Ray et al. [15], the X-ray pattern of anhydrous cement shows crystalline phases which have been identified as calcium carbonate (calcite mineral, $CaCO_3$) and calcium silicate, C_2S-alite and C_3S-belite, (at 2θ equal to 32–33°, 34° and 41.5°, respectively). In our cases, Fig. 1 reports the XRD patterns for P-C2 and HIRP-C2 samples. Here, the peaks identified, in the samples before hydration (P-C2), the presence of crystalline phases of the anhydrous cement; these crystalline phases were reduced after hydration (HIRP-C2) as a consequence of the formation of nearly amorphous CSH phase [15]. Moreover, calcium hydroxide ($Ca(OH)_2$) and ettringite (hydrated calcium aluminum sulfate mineral with formula: $Ca_6Al_2(SO_4)_3(OH)_{12}{\cdot}26H_2O$) were formed in appreciable amounts during hydration. The

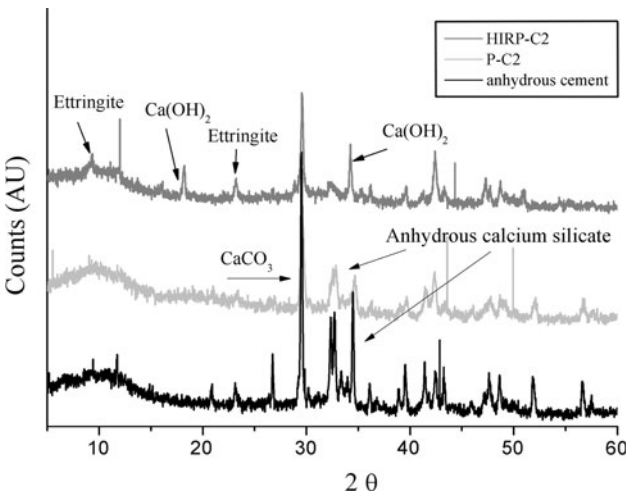

Fig. 1 XRD of anhydrous cement and selected P–C and HIRP-C samples

diffractograms of the other samples (data not reported) showed some quantitative differences in the peak intensities of the different hybrids as a consequence of the different hydration. The reason for the different amount of hydration was related to the different pore structure morphologies of the hybrid foams that, in turn, influenced the diffusion of water within the cement particles.

Microstructural analysis

SEM micrographs for HIRP-C2 foams after hydration are shown in Fig. 2. In particular, SEM micrographs at low magnification (Fig. 2a) showed a closed-celled morphology, typical of rigid polyurethane foams, with cement powder located in the struts and walls. Moreover, the cellular structure also showed the presence of open microcavities, which, as it will be shown in the following, have great influence on sound absorption property without impairing thermal insulating performances. It is important to point out that cells' structure did not change, after the hydration process, with respect to non-hydrated samples (micrograph not reported). Micrograph at higher magnification (Fig. 2b, c) evidences the typical hydration products, such as ettringite (with a morphological structure defined by Taylor as "needle like crystals" [16]), calcium silicate hydrate (gel-like flocks), and finally calcium hydroxide (with a morphological structure defined by Taylor as "plant-like crystals" [16]), proving the occurrence of the hydration reaction. It is worth of note that the micrographs were taken on an internal section of the sample, not on the external surface of the foams, denoting that the chemistry of the components, the pore morphology and the topology of the cementitious additive, allowed for the 3D "invasive" hydration of the porous material.

Water vapor permeability

Table 3 reports the water vapor permeability (μ) for Neat PUR and for selected P–C and HIRP-C samples. The μ parameter is a non-dimensional property quantifying the relative water vapor diffusion resistance of the material. In our case, the water vapor diffusion resistance of Neat PUR is very high, making this material unsuitable for application in building, for it could be responsible for muff generation, for example, and, generally, is responsible for the reduction of the comfort in the houses. Of course, the high resistance to water transport exerted by Neat PUR is due to its hydrophobic nature and the closed-celled pore structure. When the hydrophilic component (cement) was added to the hydrophobic polyurethane matrix to form the P-C4 composite foam (un-hydrated), in fact, we observed a 35 % decrease of μ with respect to the Neat PUR due to the increased average hydrophilic nature of the resulting composite material. However, only after the occurrence of the hydration reaction (in the hybrid foam, sample HIRP-C4), we observed a reduction of μ of ca. 65 % with respect

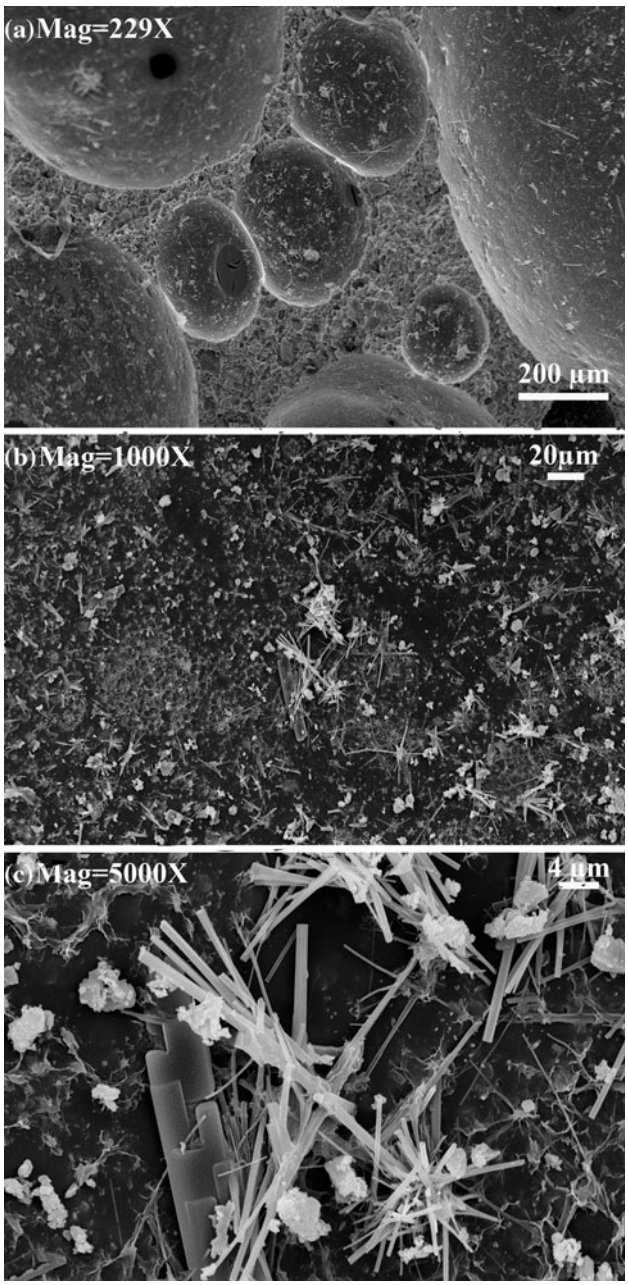

Fig. 2 SEM micrographs of selected HIRP-C samples at different magnifications: **a** ×229; **b** ×1,000; **c** ×5,000

Table 3 Water vapor transmission resistance of selected samples

Sample	μ
Neat PUR	90
P-C4	58
HIRP-C4	32

to Neat PUR. It is worth of note, here, that the value of 32 for the water vapor transmission resistance of the HIRP-C4 sample is quite similar to the ones of intrinsically hydrophilic materials utilized in building. This relevant decrease of the water vapor transmission resistance could be ascribed to the formation of the co-continuous cement phase within the polyurethane matrix as a consequence of the hydration reaction. The co-continuity, in turn, determined the occurrence of a path, accessible to water molecules, percolating throughout the hybrid. To evidence the effect of the hydration on the water vapor transmission resistance, we may observe that the composite sample (P-C4) showed a value that is an average, weighted by the relative content, of the hybrid (HIRP-C) and the Neat PUR water vapor transmission resistances.

Dimensional stability

Dimensional stability of materials is important for end use in sectors like building, where materials have to withstand different thermal and humidity conditioning during service of several tens of years. Results from dimensional stability testing on the proposed hybrid foams showed a very good dimensional stability with Δl (%) in the x, y, and z axes for the different conditioning conditions always below 0.3 %. It is worth of note that this value is one order of magnitude lower than expanded polystyrene foams typically utilized as insulating panels in building.

Adhesion test

A relevant feature of materials utilized in building is the ease of installation, which is directly related to costs of installation. One of the disadvantages of plastic insulating foams utilized for thermal insulation of buildings is the poor chemical compatibility with mortars and concrete, which hinders good adhesion and forces the use of expensive adhesive systems. In fact, adhesion tests conducted in this study evidenced very limited adhesion between Neat PUR and the mortar, with a fracture surface (more correctly, a detaching surface) coming at the interface between the mortar and the foam, proving no adhesion occurred, as it could be expected by considering the diverse chemical nature of the two materials. Conversely, the fracture surface of the HIRP-C4 sample occurred within the foamed core, hence proving that the adhesion is even stronger than the foam itself. In the case of the hybrid, in fact, the high concentration of hydrated cement distributed within the material and on the surface allows for an increased adhesion to the mortar. Photographs of Neat PUR and HIRP-C4 samples after the adhesion tests are reported in Fig. 3, where it is evident that, in the case of Neat PUR (left image in Fig. 3), fracture occurred at the interface between the mortar and the polyurethane foam, while, in the case of HIRP-C4 (right image in Fig. 3), the adhesion between the hybrid foam and the mortar was higher than the foam itself and fracture occurred within the foam and not at the interface. In particular, the strength exerted by

Fig. 3 Results of mortar-adhesion test on Neat PUR (*left*) and HIRP-C4 (*right*)

the interface of the Neat PUR-mortar system was as low as 6.8 kPa, while the strength of the interface between HIRP-C4 and the mortar was higher than 19.8 kPa, which was, in fact, the strength exerted by the core hybrid material that ruptured. It is worth of note that we also performed the adhesion test on the P-C4 material, which resulted in a relatively low improvement of adhesion with respect to Neat PUR. In this case, in effect, the strength exerted by the interface was equal to 8.4 kPa (with rupture occurring again at the interface). These results evidence the extremely important effect of hydration process on the performances of the hybrid foam, which resulted in (at least, since we observed a rupture of the foam, not of the interface, in the case of HIRP-C4) a 290 % improvement in adhesion with respect to the Neat PUR and 235 % improvement with respect to the un-hydrated material (P-C4, composite foam).

Thermal insulation properties

The results of the thermal conductivity tests performed on Neat PUR, the composites, and the hybrid systems are reported in Table 4. The results are the mean values of five determinations performed by changing the temperatures of the sample surfaces. As it was expected, the results show typical values for insulating materials in the case of the systems with the lowest densities with a decrease of the insulating performances with the increase of the density. This result is reasonable in view of the relative higher amount of conducting solid phase in higher density hybrids. However, the absolute values are still lower than that of the traditional lightweight concrete commonly used as insulator (i.e., 0.12 W/m K) [12, 17].

Acoustic properties

Sound absorption is the characteristic of a material to be able to convert the acoustic energy of sound waves into another form, often heat, which it retains to some extent, as opposed to portion of the sound energy that the material reflects or transmits. α, the sound absorption coefficient, is the absorbed fraction of incident wave energy. Typically, open-celled foams, such as flexible polyurethane foam, are good sound absorption materials. Open-celled foams, in fact, capture and absorb the sound waves because the waves dissipate their energy through friction. The dissipated mechanical energy results in heating the cells and it increases with the increase of foam porosity. In particular, it is noted [18] that the sound absorption of flexible polyurethane foams is high in high-frequency regions, but relatively weak in low frequency (100–1,000 Hz) regions, where, unfortunately, the human sensitivity is high [19]. As reported in literature, in fact, to improve the acoustic performances at low frequencies, typically, the foams are loaded with fillers in powder form [18, 19].

Rigid hybrid systems are, conversely, typically characterized by closed-celled foams, and, for this reason, they do not perform well in sound absorption, but they evidence sound absorption properties typical of resonators, where the α value is maximum at frequencies close to the resonance frequency. A resonator consists in a hole connected with a cavity, which has the role of capturing the sound waves, damping them, while the air in the hole behaves like a mass. The sound waves make the air hole to swing while the air cavity is alternatively compressed and stretched. The resulting system is the so-called spring-mass device, which has a high absorption at the resonance frequency and a low absorption at the other frequencies.

In our case, the hybrid foams showed a microstructure characterized by both closed-celled walls and by the presence of microcavity [20] that conferred it a resonator behavior in sound absorption. Figure 4 reports α values and frequency at which maximum values were attained as function of density (at equal thickness) and thickness (at equal density) for the hybrid foams in the density range of HIRP-C2. It is worth observing that the increase in density, or in thickness, induced an increase of α value toward lower frequencies (from 950 to 750 Hz). As mentioned, these properties could be attributed to the presence of open microcavity and to the large surface area at the polyurethane–cement interface, where the acoustic energy can be dissipated by interface sliding and stick–slip behavior, as observed by Liu et al. [18] on flexible polyurethane foam filled with silica fume.

The transmission of sound through a partition is described by the transmission coefficient, τ, which is defined as the ratio of transmitted to incident sound intensity, $\tau = I_2/I_1$, where I_1 is the incident sound intensity and I_2 is the radiated intensity on the other side of the partition. The Transmission Loss (TL), is the logarithmic version of the transmission

Table 4 Thermal insulating properties of Neat PU, the composite and the hybrid foams

Sample	λ (W/m K)
Neat PUR	0.028
P-C2	0.036
HIRP-C2	0.036
P-C3	0.045
HIRP-C3	0.046
P-C4	0.06
HIRP-C4	0.06
P-C7	0.11
HIRP-C7	0.11

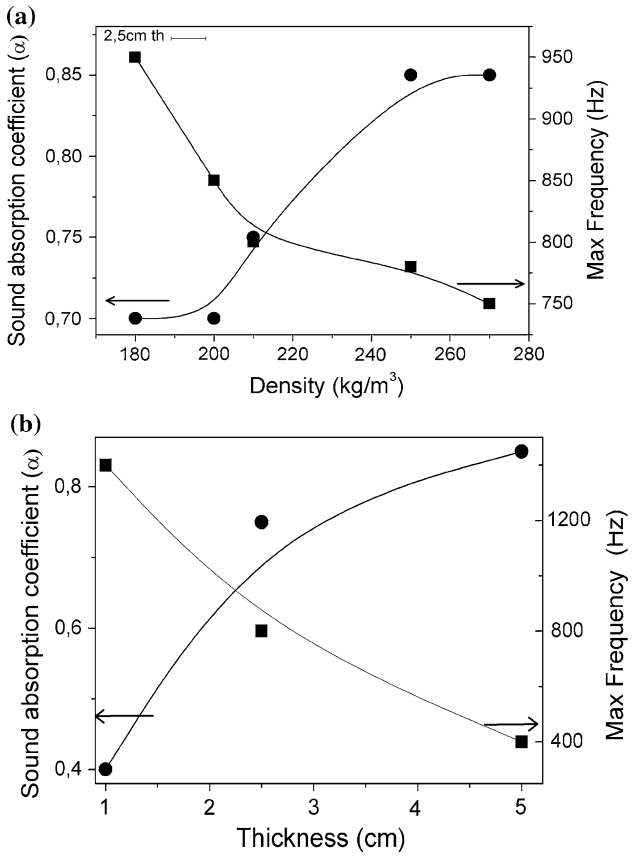

Fig. 4 Sound absorption characteristics of the proposed hybrid: **a** effect of density and **b** effect of slab thickness

coefficient in decibels and can be calculated as $TL = 10\ \log(1/\tau) = 10\ \log(I_1/I_2)$. Figure 5 reports the results of the sound insulation test in terms of the effect of the frequency on TL. For a simple thin limp material, a theoretic expression for the expected TL at frequencies below the critical frequency of the material has been derived [21]. In case of normal incident sound ($\theta = 0$), this expression reads

$$TL(0) = 20\ \log\ (fm) - 42.4,$$

where f is the frequency of the incident sound wave and m is the surface density of the panel, equal to the panel thickness times the density of the material. This equation, often referred to as the mass law, indicates that TL increases with the mass of the panel and with frequency. Figure 5 also reports the theoretic prediction of the TL according to the mass law, together with the TL of a commercial polystyrene panel, 10-cm thick with a density of 40 kg/m^3. The results of the TL test prove the hybrid to be a very efficient sound insulation structure with respect to traditional insulating material. Furthermore, as it can be explained by recalling the mass law, this performance is due to the high density of the hybrid (230 kg/m^3) with respect to the polystyrene sample, almost 6 times lower.

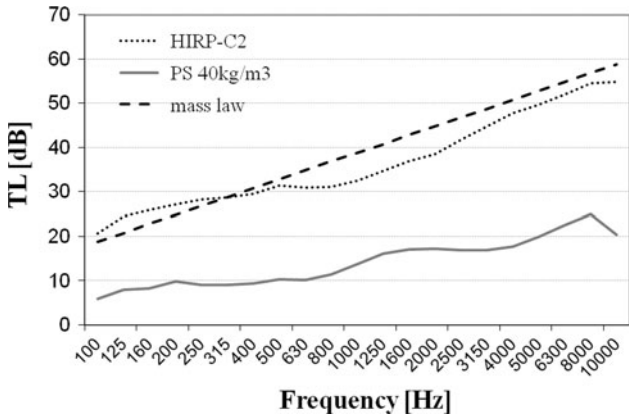

Fig. 5 Sound insulation characteristics of the proposed hybrid, comparison with PS

Thermal properties (TGA/DTGA)

TGA thermograms and corresponding derivative thermogram (DTG) curves of Neat PUR and selected composite and hybrid samples are given in Fig. 6a, while the deconvoluted DTG curve for HIRP-C-2 is reported in Fig. 6b. The TGA curves for P-C2 and HIRP-C2 have been normalized at 160 °C, to account for both physically absorbed water and chemically bound water (i.e., water present in the newly formed chemical species associated with hydration of cement particles). From the TGA of Neat PUR, two degradation steps can be observed. The first occurs in the range 200–400 °C (attaining a maximum at 321 °C) with a weight loss equal to 40 %, and the second occurs in the range 440–650 °C (attaining a maximum at 565 °C) with a 60 % mass loss. According to the literature [22–25], the first weight loss is due to the breaking of urethane links, and starts at 200 °C, leading to the formation of CO_2, alcohols, amines, aldehydes, CO, etc., and the second stage is due to the polyol decomposition. The composite and hybrid foams-based cement showed, conversely, three degradation steps: the first weight loss (18 wt% ca. for both systems) occurs in the temperature range 200–400 °C with the onset and the maximum degradation temperatures higher than Neat PUR (see Table 5). This result may be attributed to the thermal stability effect induced by the inorganic binder within the polyurethane. The second mass loss (22 wt% ca. for both systems) takes place in the range 400–540 °C with the onset and the maximum temperature values lower than Neat PUR. This result may be related to the different mechanism of PUR decomposition induced by the cementitious filler. Moreover, in this region (400–550 °C), for the hybrid foam, an additional decomposition peak was observed. In fact, the deconvoluted DTG (Fig. 6b) showed a decomposition peak at 450 °C due to the dehydration of calcium hydroxide. As reported in the discussion of XRD results, the calcium

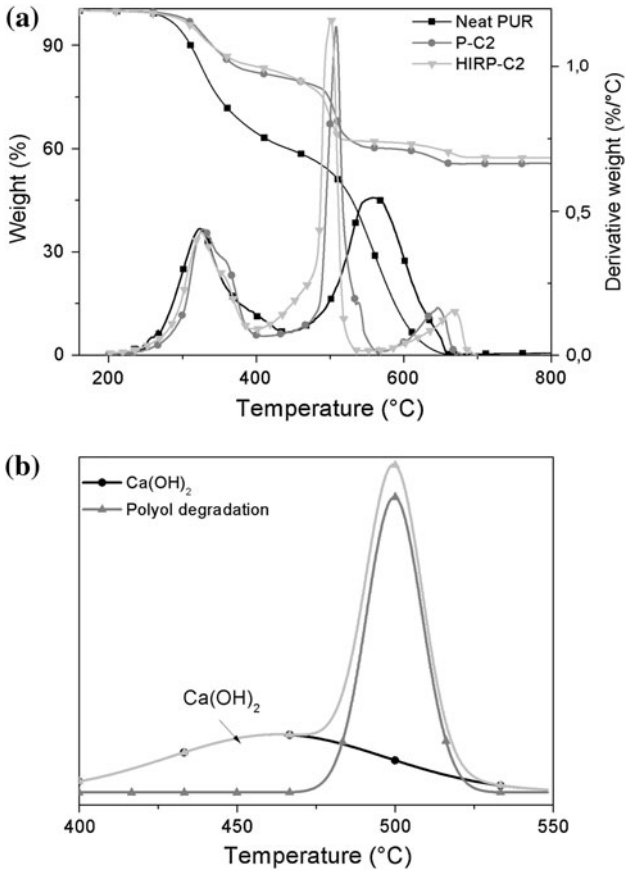

Fig. 6 **a** TGA and DTG analysis of Neat PUR and selected P–C and HIRP-C samples and **b** deconvoluted DTG in the 400–550 °C range temperature for HIRP-C2

hydroxide is a characteristic compound obtained during the cement hydration process. Finally, the third mass loss observed for both composite and hybrid foams is due to the de-carbossilation of calcium carbonate, a mineralogical compound of cement (unhydrated and hydrated), and occurs in the region 600–700 °C.

As reported in the literature [22, 26, 27], usually the presence of inorganic filler (clay, metal carbonate, etc.) in a polymeric matrix induces an increase in onset and maximum decomposition temperatures. In our case, we also observed an increase of the decomposition temperature of the urethane groups, both for the P-C2 and for the HIRP-C2 samples. However, this effect was more evident for the HIRP-C2. A possible explanation for this occurrence is that the hydrated cement phases (co-continuous phase), due to the presence of numerous OH groups of both the hydrated silicate and the hydrated aluminate, react with the surplus of unreacted isocyanate inducing an increased cross-linking density [27, 28], which is in turn responsible for the delay in the chain scission (char formation) process and the removal of the volatile decomposition products.

Table 5 Reference temperatures after TGA measurements

Sample	$T_{onset-1}$ (°C)	T_{max-1} (°C)	$T_{onset-2}$ (°C)	T_{max-2} (°C)
Neat PUR	238	321	480	565
P-C2	248	322	460	502
HIRP-C2	252	328	475	490

Table 6 Results of mechanical testing

Sample	E (MPa)	σ_c (MPa)
Neat PUR	11.3 ± 0.3	0.67 ± 0.04
P-C2	50 ± 1	1.0 ± 0.1
P-C3	61.2 ± 2	2.0 ± 0.1
P-C4	90 ± 2	3.4 ± 0.15
P-C7	260 ± 10	11.2 ± 0.5
HIRP-C2	60 ± 2	2 ± 0.1
HIRP-C3	74.5 ± 2	2.5 ± 0.2
HIRP-C4	190 ± 5	4.31 ± 0.1
HIRP-C7	306 ± 5	12.7 ± 0.2

Mechanical properties

Table 6 reports the results from compression tests in terms of the effect of the presence of cement and hydration on Young modulus and compressive strength of polyurethane-based materials. As it can be expected, the presence of the cementitious filler increases the stiffness of the polyurethane without decreasing the strength (compare Neat PUR and P-C2). Furthermore, among the composites (P–C samples) and the hybrid (HIRP-C samples), both the stiffness and the strength of the materials increase with increasing foam density. The elastic modulus, for example, increases from ca. 50 to 260 MPa with density increasing from 230 to 750 kg/m^3 for the case of composite foams, while, for the case of the hybrid foams, elastic modulus increases from 60 to 306 MPa ca. when the density increases from 200 to 800 kg/m^3. It is worth of note, in this context, the effect of hydration by comparing composite foams with hybrid foams at the same density. In effect, the proved occurrence of hydration and co-continuity of the inorganic phase allowed for an increase of compressive mechanical properties with stiffness actually doubling, for example, in the case of P-C4 and HIRP-C4 samples. Compressive strength increased with the occurrence of hydration by 100 % in the case of samples with densities of ca. 200 kg/m^3 and by 25 % in the case of 400 kg/m^3 densities.

Conclusions

The functional and mechanical properties of the different materials reported in this work evidenced a quite extensive

effect of the occurrence of co-continuity of the organic and the hydrated inorganic phases, as a result of cement hydration. As it has been proved by XRD and degree of hydration data, the exposure of the cement-filled polyurethane to water molecules determines the formation of the typical hydrated products of the cement reactions. In turn, these products, in specific concentration and topology, were able to form a percolating structure within the polyurethane matrix (co-continuity). The effects of this co-continuous structure, in comparison with neat polyurethane and unhydrated cement-filled polyurethane, were relevant on

- water vapor permeability: percolating hydrophilic cement particles allow for a continuous path for water molecules within the polyurethane foam;
- dimensional stability: the inorganic structure prevails in determining the behavior of the hybrid when subjected to environmental stimuli;
- adhesion to mortars: the presence of the inorganic material within the hybrid enhances the chemical compatibility to inorganic binders;
- acoustic properties: both insulation and absorption increases for the increased density of the cement-filled polyurethane with respect to neat polyurethane and for the formation of micro cavities within the closed cell walls;
- thermal stability: the presence of the hydrated cement allows for an increase of thermal stability possibly due to increased crosslinking density of polyurethane;
- mechanical properties: as in the case of dimensional stability, a great effect has been observed when the cement particles touch each other (co-continuity) and becomes therefore able to sustain loads.

Finally, it has been shown how the occurrence of the hydration of the cement phase within a polyurethane–cement composite foams allowed for the achievement of a new class of materials, namely HIRP-C hybrid foam.

References

1. Hilyard NC, Cunningham A (eds) (1994) Low density cellular plastics physical basis of behavior. Chapman and Hall, New York
2. Randall D, Lee S (eds) (2002) The polyurethanes book—Huntsman polyurethane. Wiley, New York
3. Kim SH, Park HC, Jeong HM, Kim BK (2010) J Mater Sci 45:2675. doi:10.1007/s10853-010-4248-3
4. Hararak B, Prakymoramas N, Rungseesantivanon W, Thamumjitr D (2010) In: Suttiruengwong S, Sricharussin W (eds) Advanced material research-functionalized and sensing materials. Trans Tech Publishing, Bangkok, Thailand
5. Nikje MMA (2010) Polym Eng Sci 50:468
6. Kang JW, Kim JM, Kim MS, Kim YH, Kim WN, Jang W, Shin DS (2009) Macromol Res 17:856
7. Yuan J, Shi SQ (2009) J Appl Polym Sci 113:2902
8. Tien YI, Wei KH (2002) J Appl Polym Sci 86:1741
9. Novak I, Krupa I, Chodak I (2002) J Mater Sci Lett 21:1039
10. Verdolotti L, Di Maio E, Lavorgna M, Iannace S (2006) A foamed polymer-inorganic binder hybrid material controller density and morphology, method for its preparation and uses thereof. WO2008/007187
11. Verdolotti L, Di Maio E, Lavorgna M, Iannace S (2008) J Appl Polym Sci 107:1
12. Verdolotti L, Di Maio E, Forte G, Lavorgna M, Iannace S (2010) J Mater Sci 45:3388. doi:10.1007/s10853-010-4416-5
13. Escalante-Garcia JI, Sharp JH (1998) Cem Concr Res 28:1245
14. Iñiguez-Sánchez CA, Gómez-Zamorano LY, Alonso MC (2012) J Mater Sci 41:3639. doi:10.1007/s10853-011-6210-4
15. Ray I, Gupta AP, Biswas M (1996) Cem Concr Compos 18:343
16. Taylor HFW (1997) In: Cement chemistry, 2nd edn. Thomas Telford Publishing, London
17. Sarier N, Onder E (2008) Thermochim Acta 452:149
18. Liu T, Mao L, Liu F, Jiang W, He Z, Fang P (2011) Wuhan Univ J Nat Sci 16:029
19. Bo L, Hong Z, Guangsu H (2007) J Mater Sci 42:199. doi:10.1007/s10853-006-1052-1
20. Iannace G, Masullo M, Di Maio E, Verdolotti L (2009) RIA 33:49
21. Beranek LL (1971) Noise and vibration control. McGraw-Hill Book Company, New York
22. Verdolotti L, Salerno A, Lamanna R, Nunziata A, Netti P, Iannace S (2011) Microporous Mesoporous Mater 151:79
23. Modesti M, Zanella L, Lorenzetti A, Bertani R, Gleria M (2005) Polym Degrad Stab 87:287
24. Kramer RH, Zammarano M, Linteris GT, Gedde UW, Gilman JW (2010) Polym Degrad Stab 95:1115
25. Lorenzetti A, Modesti M, Besco S, Hrelja D, Donadi S (2011) Polym Degrad Stab 96:1455
26. Siengchin S, Karger-Kocsis J, Psarras GC, Thomann R (2008) J Appl Polym Sci 110:1613
27. Mahfuz H, Rangari VK, Islam MS, Jeelani S (2004) Compos A 35:453
28. Petrovic ZS (2008) Polym Rev 48:109